ELSEVIER

Nuclear Instruments and Methods in Physics Research A 464 (2001) 271–277

NUCLEAR INSTRUMENTS & METHODS IN PHYSICS RESEARCH Section A

www.elsevier.nl/locate/nima

Matching final focus to distributed radiator target requirements with skew quadrupoles

A.W. Molvik*, J.J. Barnard

Heavy-Ion Fusion Virtual National Laboratory, Lawrence Livermore National Laboratory, P.O. Box 808, L-645, Livermore, CA 94550, USA

Abstract

We demonstrate that ion-beam elliptical focal spots can be rotated with skew quadrupoles, by arbitrary angles, to map appropriately onto annular rings at either end of distributed-radiator heavy-ion fusion targets. The rotation is accompanied by an increase in the area, a variation in the ellipticity, and a shift in the axial location of the beam focal spot, all of which are small enough that they may be acceptable. Possible further optimizations are discussed.

PACS: 52.58.Hm; 41.85.Lc

Keywords: Skew quadrupole; Final focus; Distributed radiator target; Moment code; Heavy-ion fusion

1. Introduction

Recent distributed-radiator heavy-ion-fusion target designs [1,2] require that incident ion beams with elliptical cross-sections map out annular rings at either end of a hohlraum, Fig. 1. Fusion driver induction accelerators will transport many beamlets by the use of alternating gradient electrostatic or magnetic quadrupoles. These quadrupoles deliver beams with the principle axes of their elliptical cross-section oriented at 0° and 90° (or equivalently $\pm 45^\circ$). These beams could, for example, be focused to four spots with uniform azimuthal spacing. If these pairs of beamlets can each be rotated by arbitrary angles of up to $\pm 45^\circ$, then beams can be focused to any angle on the end of the hohlraum.

For this paper, we use a moment code to evaluate the beam focal spot rotation and changes in spot area and ellipticity produced by magnetic quadrupoles that are rotated to a skewed angle. We find that we can rotate beamlet elliptical–focal spots to arbitrary angles. However, when the transverse x and y emittances are equal, the smallest area focal spot is circular; then uniform illumination can be achieved with overlapping focal spots, without requiring beamlet rotation if a large number of beamlets are used. Although we evaluate focusing ion beams onto a specific target design, these focal spot manipulations are more general. The techniques described here are capable of illuminating other target shapes with arbitrary intensity distributions, limited only by the minimum focal spot size and shape and by the number of beams.

*Corresponding author. Tel.: +1 925 422 9817; fax +1 925 424 6401.

E-mail address: molvik1@llnl.gov (A.W. Molvik).

0168-9002/01/$ - see front matter
PII: S0168-9002(01)00047-X

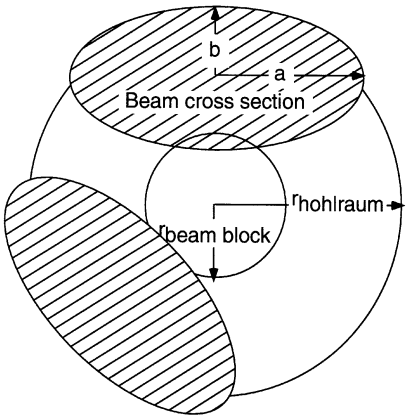

Fig. 1. The dimensions of each beam focal spot must fit within the annular region between the hohlraum radius and the beam block radius (which protects the capsule from impinging beams). With multiple beams, the annular region can be uniformly illuminated by displacing and rotating each beam focal spot, as is indicated for two beams.

We rotate the focal spot by means of one skewed quadrupole magnet, whose axes are off the usual 0°, 90° rotation angle (see, for example, Ref. [3]). We demonstrate the feasibility of this approach by using a concrete example of a final focus layout that would meet the target requirements of a distributed radiator target. We emphasize that our example is not optimized, but nevertheless demonstrates the existence of a straightforward method of achieving the needed ellipticity and rotation angle. Our purpose and conclusions differ from those of Neuffer, who examined $\pm 90^\circ$ rotations achieved by means of skewed quadrupoles, and developed necessary and sufficient conditions to completely interchange the x and y phase spaces [4]. Our requirement is less restrictive, namely that the skew quadrupole not cause a significant increase in the beam power falling outside the usable, elliptical focal spot.

2. Physics of moment code

In Ref. [5], a set of moment equations for the ten second order moments ($\langle x^2\rangle$, $\langle xx'\rangle$, $\langle x'^2\rangle$, $\langle y^2\rangle$, $\langle yy'\rangle$, $\langle y'^2\rangle$, $\langle xy\rangle$, $\langle xy'\rangle$, $\langle x'y\rangle$, $\langle x'y'\rangle$) were derived which generalized the traditional envelope equations for upright ellipses. Here $\langle\rangle$ indicates average over the distribution function, at a fixed slice of the beam in the longitudinal coordinate z, and x and y are the horizontal and vertical coordinates, respectively, in the fixed laboratory frame. Also, prime ($'$) indicates derivative with respect to z. The basic assumptions were: the beam density is uniform, with elliptical cross-section, and it is subject to forces that are linear in the transverse cartesian coordinates x and y. The axes of the ellipse, however, are not necessarily aligned with the x and y axes (or the axes of the skew quad). The generalized equations allow $x-y$ coupling. That is, in the x-equation of motion, for example, a term proportional to the y-coordinate of the particle (arising from the focusing force of a skew quad or the space charge force of a rotated beam) is allowed. Further, finite angular momentum of the beam is allowed. The set of equations no longer conserves x- or y-emittances ε_x, ε_y, but two conserved generalized emittances take the place of ε_x and ε_y [6]. Although, the equations were derived for a uniform density beam, as with the traditional envelope equations, they are expected to give a good estimate of beam behavior for less idealized beams as well. Effects of dispersion in bends, chromaticity in quadrupoles, image charges, non-uniform space-charge distributions, and any accelerator imperfections that would cause increase of the generalized emittances are not included in this set of equations. However, we expect the qualitative behavior of the solutions to be unaltered when these effects are included, at the same level of confidence that the envelope equations are a good qualitative predictor of behavior of beams with upright beam ellipses. Also, for simplicity we have assumed a sharp onset of a fully neutralized beam in the target chamber. Deviations from this assumption can be treated by prescribing a finite transition region over which the neutralization occurs. Non-linearities arising from inhomogeneous electron distributions are beyond the scope of this paper and must be treated with particle codes. The equations in Ref. [5] were numerically integrated, assuming hard-edge field configurations for the quadrupoles. The results are described below.

3. Required rotation angles

For N_b beam focal spots spaced uniformly around a ring, the change in rotation angle $\Delta\alpha$ between adjacent beams is given by $\Delta\alpha = 360^\circ/N_b$. Since the beams already come in two orientations separated by 90°, by rotating each of two such beams towards each other by an angle α, the remaining angle between them will be $\Delta\alpha = (90^\circ - 2\alpha)$. The relation between N_b and α is then

$$N_b = (360^\circ)/(90^\circ - 2\alpha).$$

N_b is tabulated in Table 1 for various maximum rotation angles α. We see that with rotation angles of up to $\pm 45^\circ$, any number of beams can be evenly spaced azimuthally. In the target modeling, 16 evenly-spaced elliptical beams were deemed to provide adequately uniform illumination. This requires $\pm 33.75^\circ$ rotations.

It might be expected that $\theta = 45^\circ$ would be the optimum skew angle, because this would line up the cusps of the skewed quadrupole with the major and minor axes of an elliptical beam. The $qv\times B$ force would then rotate the major axis, however, little or no rotation would result with a circular beam. The moment code showed that this conjecture is wrong: the focal spot rotation was independent of whether the beam was circular or elliptical at the skewed quadrupole, and larger rotations resulted for skew quadrupole angles greater than 45°. Our present understanding is that the skew quadrupoles squeeze the beam ellipse towards the skew quadrupole angle from the initial starting orientation of 0° or 90°. In other words, we deform the beams with forces that do not lie in either the 0° or 90° planes. This model fits our computational results better than does another conjecture—that we need to supply specific net angular momentum to rotate the beam by up to a few millimeters at the focal spot, several meters away. For example, the beam does obtain larger angular momentum if the skew quad is placed where the beam has higher ellipticity, as expected, but the focal spot rotation is unchanged, as mentioned above. We find that the higher the magnetic field in the skew quadrupole, the larger the angle of rotation, until saturation effects set in.

Table 1
Beam rotation angle

α (°)	$\Delta\alpha$ gap(°)	N_b
0	90	4
22.5	45	8
30	30	12
33.75	22.5	16
35	20	18
37.5	15	24
40	10	36
45	0	∞

4. Model setup

We selected a final focus array of quadrupole magnets that was designed for 96 beamlets per end of the hohlraum [7]. Each beam had a perveance of 1.581×10^{-4}, a rigidity of 49.59 T m, and an initial normalized emittance of 1.424 mm mrad. The magnet locations, field gradients and the beam envelopes through the lens train to the focal spot are shown in Fig. 2(a) and (b) and parameters listed in Table 2. The initial conditions were those of a matched beam for a lattice consisting of the first two (non-skew) quadrupoles. We assume 100% neutralization of the beam for $z > 16.4\,m$, from the point where the a and b envelopes become nearly straight lines to the target (where $a \equiv 2\langle x^2\rangle^{1/2}$ and $b \equiv 2\langle y^2\rangle^{1/2}$ are measured in the [unrotated] lab frame). We tried several locations for one or more skew quadrupoles, labeled with 1–3. With equal x and y emittances, the focal spot was circular. We made it elliptical by changing the magnetic fields of the last two quadrupoles by $\sim$0.1%. This produced two elliptical foci, rotated by 90° relative to each other as shown in a blow-up of the focus region Fig. 2(c), and each with a spot area somewhat greater than the optimum focus, Fig. 2(d). For this case, the minimum area focus was circular with an area indicated by the bottom square data point that lies below the lines. For other beam rotations, two displaced minimum area elliptical foci exist.

In evaluating the effect of a skewed quadrupole we chose a fixed distance of 20.6 m at which to

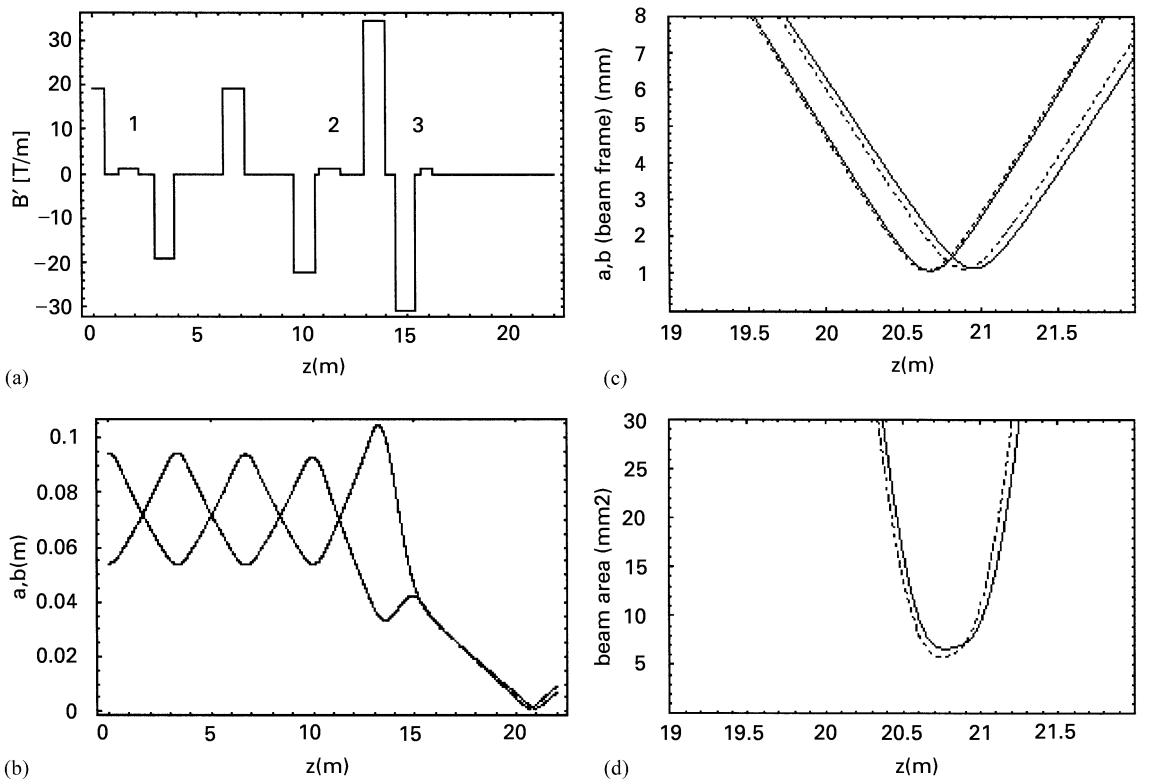

Fig. 2. (a) Final focus lens train: the 3 locations used for $\theta = 45^\circ$ skew quadrupoles are numbered. They are powered one at a time for Figs. 3 and 4. (b) Beam envelopes in 0° and 90° planes (the laboratory frame) with 100% neutralized transport, after about 16 m, over the straight-line portion of the nearly overlapping trajectories. (c) The beam envelopes are expanded near focus. Dashed lines are without, solid lines with skew quadrupoles. (d) The beam area is expanded near focus.

Table 2
Parameters used in Fig. 2. "Var." indicates the possible sections that contained skew quads, in this study. The rotation angle and field gradient of the skew quad were varied. Sections with 0 field gradient are drift sections

Section number	1	2	3	4	5	6	7	8	9	10
Section length (m)	0.504	0.672	1.008	0.672	1.008	2.352	1.008	2.352	1.008	0.2
Field gradient (T/m)	18.91	0	Var.	0	−18.91	0	18.91	0	−22.40	0
Assumed neutralization on fraction	0	0	0	0	0	0	0	0	0	0
Assumed rotation angle (rad)	0	0	Var.	0	0	0	0	0	0	0

Section number	11	12	13	14	15	16	17	18	19
Section length (m)	1.008	1.144	1.008	0.473	1.008	0.2	0.583	0.2	5.592
Field gradient (T/m)	Var.	0	34.38	0	−30.64	0	Var.	0	0
Assumed neutralization on fraction	0	0	0	0	0	0	0	0	1
Assumed rotation angle (rad)	Var.	0	0	0	0	0	Var.	0	0

evaluate the angle, shape, and area of the focal spot. This distance is measured from the center of the first focusing magnet included in the simulation, Fig. 2(a), to near the first elliptical focus point, Fig. 2(c). In addition we evaluate these parameters at the distance of the minimum spot area. This choice reflects the operating restrictions of the currently planned, closely coupled arrays of

quadrupole magnetic lenses, in which the magnetic flux is shared between four adjacent beams to minimize the size and cost of the superconducting magnets (For similar pulsed magnet arrays, see Ref. [8]). With such systems, we cannot vary the focusing strength for one beam without affecting its neighbors. The skew quadrupoles use much lower magnetic fields so that a surrounding iron tube can magnetically shield each, and therefore each can be varied independently of its neighbors. In addition to requiring that the skew quadrupole fields be $\ll 2\,\mathrm{T}$, the iron around each skew quadrupole must also be outside of the higher fringe field of the main quadrupoles. As suggested earlier, we found that the distance to the focal spot varied slightly with the strength of the skew quadrupole.

5. Results

We first used skew quadrupoles, rotated by 45°, and located at the three locations shown in Fig. 2, after the first optic, between the fourth and fifth, and after the sixth or final quadrupole lens. The focal spot area A at 20.6 m, the ratio of the major to minor radius a/b (in the rotated frame in which the coordinate axes are aligned with the beam axes), and the minimum focal spot area at optimum focus are plotted in Fig. 3, versus the rotation angle α of the focal spot. We find that the location of $\theta = 45^\circ$ skew quadrupoles within the lens train has little or no effect on their effectiveness, as A, a/b, and z vary with the rotation angle α, independent of the skew quadrupole locations, labeled 1–3. We obtained the same result by operating multiple 45° skew quadrupoles simultaneously, the results shown are for one at a time. (The point, at $\alpha = 0^\circ$ with smaller area and $a/b = 1$, is for a circular focal spot with skew quadrupoles turned off.) With a single skew quadrupole at $\theta = 45^\circ$, the practical maximum angle of rotation is $\alpha = \pm 25-30^\circ$. Beyond that angle the area and a/b increase rapidly, and focal point shifts further. From Table 1, this restricts us to no more than 12 elliptical evenly spaced beamlet spots on the target.

Focal spot rotations to larger angles can be achieved by using a skew quadrupole rotated to $\theta = 65^\circ$ at location 1. Then the accessible range of angles is from -5° to 45°, or even -10° to 50°, Fig. 4. By adding a second skew quadrupole at $\theta = -65^\circ$ and powering one at time, the entire range of focal spot angles can be accessed over the range of $\pm 45^\circ$, and from Table 1, any number of beamlets can be evenly spaced azimuthally around the target.

From the point of view of minimizing the spot size on the target, circular to slightly elliptical focal spots offer the minimum area if the transverse emittances ε_x and ε_y are nearly equal as we would normally expect with a linac. But after acceleration, the beams are bent around arcs to impinge on the target from two sides. These bends are expected to yield non-equal transverse emittances, which will optimally focus to an elliptical spot. If the beam cross-sections are sufficiently elliptical at

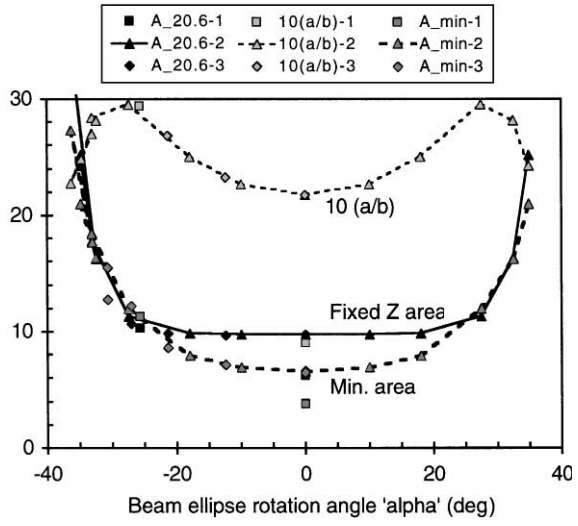

Fig. 3. With a $\theta = 45^\circ$ skew quadrupole, we plot parameters versus the rotation angle of the focal spot: The upper dashed line indicates the shape, 10 (a/b), of the focal spot at 20.6 m. The solid line indicates the area (mm^2) at a fixed location, z= 20.6 m. The heavy-dashed line indicates the minimum area (mm^2) of the focal spot, at the optimum distance. The shape of the point, and the final digit in the legend, indicate which of 3 quadrupole positions from Fig. 2(a) is used, 1(square), 2(triangle), or 3(diamond). This shows that the skew quadrupole location is not critical.

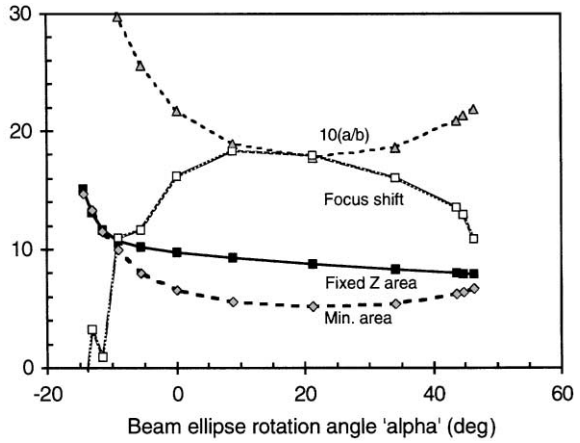

Fig. 4. Similar to Fig. 3, but with a $\theta = 65^\circ$ skew quadrupole, we plot parameters versus the rotation angle of the focal spot: The upper dashed line indicates the shape, 10 (a/b), of the focal spot at 20.6 m, with a and b measured in the rotated frame. The solid line with open squares indicates the shift of the optimum focus from 20.6 m (in cm). The solid line with filled square data points shows the fixed z area (mm^2). The lower heavy-dashed line indicates the minimum area (mm^2) of the focal spot, at the optimum distance.

focus, then techniques similar to those described here can rotate each beamlet to the appropriate angle on the target.

In this paper, where we started with equal x and y transverse emittances, the only way we found to make the focal spot more elliptical was to keep the diameter constant in one direction while we increased the diameter in the orthogonal direction at focus. This, of course, does not conserve the focal spot area. If we have $\leqslant 16$ beams, elliptical cross-sections with the proper rotation are believed necessary to allow the focal spots to overlap for more uniform illumination. If, however, we have many more than 16 beams per side, then circular focal spots, which do not require rotation, would overlap sufficiently to provide uniform illumination.

6. Future optimizations

We tried several methods of optimizing further. We reoptimized the entire lens train to produce an elliptical beam spot at the desired distance. This produced a single minimum area focal spot, rather than the two shown in Fig. 2(c). Rather than the nearly circular beams approaching focus and becoming elliptical only very near focus, as shown in Fig. 2(b) and (c); this case had an elliptical beam through most of region following the final quadrupole. The convergence angles of the two transverse beam planes differed by nearly a factor of two. Then either side of focus, the major and minor elliptical axes interchanged. This resulted in rapid changes in the rotation angle, which coupled with shifts in the focal length, so we did not obtain predictable rotations that varied nearly linearly with the quadrupole field magnitude. Instead, the rotations varied faster than linearly. This optimization reduced the maximum beam diameter at the fourth quadrupole, allowing it to have a smaller diameter. Some reduction in the focusing field requirement is also expected.

We also tried to pick the fixed distance closer to the minimum focal spot than shown by the focus shift (centimeters) in Fig. 4. We found that the beam became nearly circular at this distance, and the rotation angle varied nonlinearly with the quadrupole field.

For future work, we expect that we could further optimize by adding additional skewed, and possibly non-skewed, low-field quadrupole magnets that are shielded by iron tubes. Non-skewed quadrupoles should allow adjusting the focal length to prevent variation with rotation angle. This might enable us to obtain predictable rotations with the elliptically optimized beam discussed above. We speculate that additional quadrupoles might allow the ellipticity to also be held constant as the rotation angle is varied. Shielded crossed-dipole magnets would allow fine-tuning the aiming of the focal spot on the target. We chose location 1, furthest from the target for the 65 skew quadrupole calculations shown in Fig. 4. This location was chosen to minimize the neutron flux at the magnet. However, since this is a low-field and relatively inexpensive magnet, the apparently undesirable approach of placing it near location 3 (between the final optic and the target) might also be worth investigating. This would allow it to be part of the shielding for the main quadrupole lenses.

In this work, we demonstrated the principles of rotating ion-beam elliptical focal spots with skew quadrupoles. We found that we could achieve arbitrary angles of rotation, to map appropriately onto annular rings at either end of distributed-radiator heavy-ion fusion targets. These techniques could be generalized to produce a wide variety of arbitrary power distributions for other target designs. This feasibility demonstration is adequate for our present needs. If beamlet rotation is necessary in the future, then the suggestions above may help to ameliorate the problem areas. These are: an increase in the area, a variation in the ellipticity, and a shift in the axial location of the beam focal spot; but all of which are small enough that they may be acceptable.

Acknowledgements

We would like to thank Roger Bangerter for useful discussions regarding skew quads and final focus optimizations, and an anonymous referee for making useful suggestions to clarify this paper.

This work was performed under the auspices of the US Department of Energy by University of California Lawrence Livermore National Laboratory under contract No. W-7405-Eng-48.

References

[1] D.A. Callahan-Miller, M. Tabak, Nucl. Fusion 39 (1999) 883.
[2] D.A. Callahan-Miller, M. Tabak, Nucl. Fusion 39 (1999) 1547.
[3] D.A. Edwards, M.J. Syphers, The Physics of High Energy Accelerators, Wiley, New York, 1993.(Chapter 5)
[4] D. Neuffer, Insertion of skew quadrupoles to exchange $x - x'$ and $y - y'$ phase spaces, Proceedings of Heavy Ion Fusion Workshop, Argonne National Laboratory, 1978.
[5] J.J. Barnard, Emittance growth from rotated quadrupoles, Proceedings of the Particle Accelerator Conference, Dallas, TX, May 1–5, 1995, Vol. 5, 1996, p. 3241.
[6] R.A. Kishek, J.J. Barnard, Effects of quadrupoles rotations on the transport of space charge dominated beams: theory and simulations comparing linacs with circular machines, Proceedings of the 1999 Particle Accelerator Conference, NY, March 29–April 2, 1999, p. 1761.
[7] E.P. Lee, Private communication, 1999.
[8] A. Faltens, N.Y. Li, G. Ritchie, D. Shuman, A pulsed elliptical quadrupole array for transport of multiple high current beams, Proceedings of the 1999 Particle Accelerator Conference, New York, 1999, p. 3339, Available at http://pac99.bnl.gov/.